CLOSED ORBIT CORRECTION AND BEAM DYNAMICS ISSUES AT ALBA

M. Muñoz, D. Einfeld, T. F. Günzel*, CELLS, PO Box 68, 08193 Bellaterra, Spain.

Abstract

ALBA is a 3 GeV light source being built in Spain. The light source should be operational in 2010.The lattice for the storage ring is now finalized. The basic cells is an extended DBA-like structure with finite dispersion in the straight sections, providing low emittance (under 5nm×rad), small beam cross sections at the source points (less than 150 μm horizontal and 10 μm vertical), and a large number of straight sections (4 of 8 m, 12 of 4.2 m and 8 of 2.6 m). In this paper we review the lattice with special emphasis in the flexibility of the lattice, closed orbit correction and resistive wall instabilities

INTRODUCTION

ALBA is a 3^{rd} generation light source under construction close to Barcelona, Spain. The lattice chosen offers a good compromise between a large numbers of straight section avaliable for insertion devices (3 of 8 m and 12 of 4.2 m are free for IDs), beam size at the light sources (130 μm×8 μm in the 4.2 m straight sections) with a relatively small circumference (268 m) for the energy (3 GeV) of the storage ring. To reach this performance, several compromises were adopted in the design of the lattice, in order to free as much space as possible for ID and to reduce the beam sizes: including that most of the vertical focusing takes place in the bending magnets, with a large integrated gradient; only doublets of quadrupole magnets in most of the straight sections and corrector magnets integrated in the sextupoles. This compromises raised some questions about the lattice flexibility, including the possibility to move the working point and to compensate the β-beating, and about the performance of the correction system. In this paper we examine this two problems, and the solutions adopted, as well as the effect of the multipoles and the first estimation of the resistive wall instability.

LATTICE

The lattice adopted for ALBA is a based in a DBA structure. The bending magnets include a moderately high gradient (5.6 T/m), and most of the vertical focusing takes place in them. In order to reduce the emittance, some dispersion is allowed to leak in the straight sections, providing an emittance of 4.5 nm×rad. Figure 1 shows the optical functions for one quarter of the ring. The main parameters of the machine are show in table 1.

Due to the relatively low chromaticity and the use of nine families of sextupoles, it is possbible to obtain a large dynamic aperture. The energy acceptance of the lattice is also good, providing, even in presence of coupling errors and realistic physical apertures, a larger acceptance than the 3% provided by the radio frequency system. This will provide a Touschek lifetime over 40 hours at a current of 400 mA Figure 2 shows the core of the dynamic aperture and frequency map for the ideal lattice.

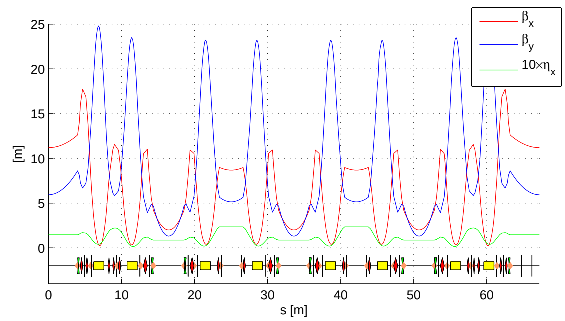

Figure 1: Optical functions for 1/4th of the ring.

Table 1: Parameters of the storage ring

Circumference	268.8 m
Energy	3 GeV
Emittance	4.5 nm×rad
Tunes	(18.18, 8.37)
Natural Chromaticity	(-39, -27)
Relative Energy Spread	1.05×10^{-3}
Momentum Compaction Factor	8.8×10^{-4}
Damping Partition Numbers	(1.3, 1, 1.7)
Energy Loss per Turn	1.007 keV

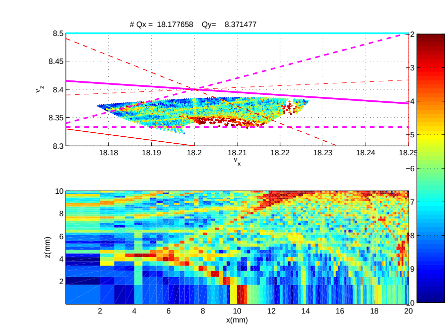

Figure 2: Dynamic aperture and frequency map for the ideal lattice.

* on leave from ESRF, Grenoble, France

LATTICE FLEXIBILITY

To move the working point, the lattice has been fitted to a set of working point in a range of tune of ± 0.5 units using the MAD code, using all the quadrupoles, while preserving similar optical functions that the reference working point. That has allow the creation of a look up table of the settings of the quadrupoles in function of the change of tune. It was also possible to match the lattice to different optics mode without changing the gradient of the dipoles, using only the quadrupole power supplies. For example, it is possible to match the lattice to an achromatic mode keeping similar beam sizes in the medium straight sections, with a good dynamic aperture and energy acceptance.

The performace obtained in the β-beat correction is show in 3. A random distribution of errors in the gradient in the quads (with $\sigma = 1 \times 10^{-3}$ m^{-2}) and bending magnets (with $\sigma = 2.5 \times 10^{-3}$ m^{-2}), with a β-beat up to 70%, with a shift in the tunes of (0.025, -0.02). To compensate this, a method based in response matrices and SVD has been developed, using two response matrices, one for the change of the β-functions at the quadrupoles in function of the change of the quadrupoles gradient ($\Delta\beta_j^{x,y}/\Delta K_i$), and one for the changes of the tunes in function of the change of the quadrupoles gradient ($\Delta Q_{x,y}/\Delta K_i$). The matrices are inverted using SVD, with the optical functions compensated first, and then the tunes. After a few iterations of this method, the optical functions and the tunes are corrected, with a remanent β-beat under 3%. This same procedure has been applied to compensate the effect of the insertion devices.

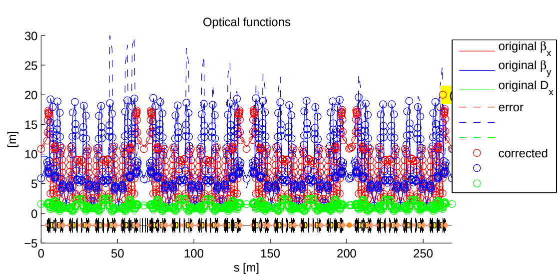

Figure 3: Example of beta beat compensation.

EFFECT OF THE MULTIPOLES

Realistic values of the systematic and random multipoles expected in the quadrupoles and in the bending magnets are now avaliable, and they are summarized in tables 2. This values have been introduced in the model, using the Tracy-2 simulation code. The main effect is the sextupolar contribution of the dipole, that increases the vertical chromaticity in one unit. However, the dynamic aperture is still good, as show in figure 4, and we can conclude that the effect of the multipoles is small.

Table 2: Multipolar components of the quadrupoles and dipoles, expressed as the magnetic field ratio at a radius of 20 mm.

Coefficient	**Quadrupole** B_n/B_2	**Dipole** B_n/B_1
Sextupole	$< 5 \times 10^{-4}$	6×10^{-4}
Octupole	$< 5 \times 10^{-4}$	3×10^{-4}
Decapole	$< 2 \times 10^{-4}$	7×10^{-5}
Dodecapole	3×10^{-4}	

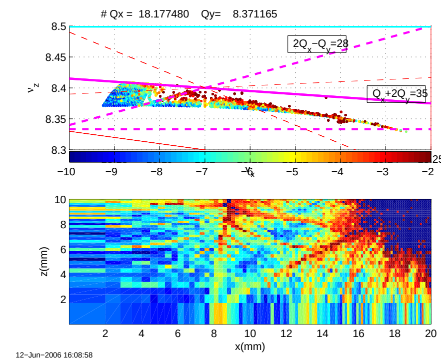

Figure 4: Dynamic aperture and frequency map including the effect of the multipoles.

CLOSED ORBIT CORRECTION

The design of the lattice provides space for 120 Beam Position Monitors, and also for 120 corrector coils in each plane in the sextupoles. Analysis of the response matrices and of the SVD singular values shows that this number can be reduced to 88 without any degradation in the performance of the correction. Figures 5 and 6 shows the required corrector strength and the distribution of the correctors in the machine, for a realistic distribution of errors (girder-to-girder alignment error of 150 μm, element-to-girder alignment error of 50 μm, rotation error of 100 μrad) for 200 sample cases. The maximum strength required is well under the limits of the one provided by the correctors (1 mrad). With this settings the residual orbit is well under the submicron level at the BPMs, and the coupling is corrected to values under 0.5%

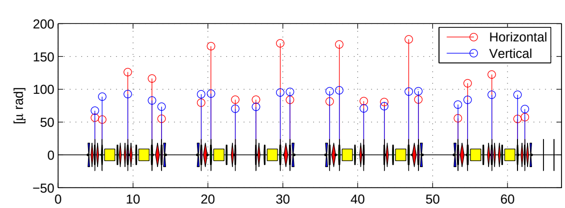

Figure 5: Distribution of the RMS values of the correctors, for 200 sample cases, for correcting a realistic distribution of errors.

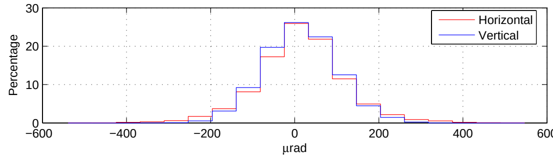

Figure 6: Histogram of the distribution of the strength of the correctors for 200 sample cases, for correcting a realistic distribution of errors.

RESISTIVE WALL INSTABILITY

Two opposite assumptions for the vacuum system configuration were made under the perspective that the true resistive wall impedance will always be inbetween these 2 cases. The first one corresponds to the vacuum system at commissioning status (best case) with no low-gap chamber. The second corresponds to all straight sections equipped with stainless steel chambers of 8mm gap (worst case). Furthermore, the impedance of the low-gap chambers was weighted by the local value of the corresponding β-function and not calculated by $<\beta>= C/(2\pi\nu_\beta)$ (C circumference, ν_β betatron tune). The effect of finite thickness of the vacuum chamber wall was neglected. Under the assumption that the vacuum chambers are sufficiently flat to be considered as two parallel plates, the form factors given in [1] can be used. Then with the use of the formula (with $Z_0 = 377\ \Omega$, σ as resistivity of the chamber wall material, a as vertical half extension of the chamber, ω as angular frequency, with $F = \pi^2/12$ (vert.) res. $\pi^2/24$ (hor.) as form factor, L as length of the element and $\sigma_\tau = 15.6$ps as bunch length) :

$$Z_\perp = (sign(\omega) + i)F\frac{Z_0 L}{2\pi a^3}\sqrt{\frac{2c}{\sigma Z_0 \omega}} \qquad (1)$$

the following effective impedances in table 3 could be obtained. An adapted version of the code ZAP[2] was used to calculate the multibunch resistive wall thresholds in order to cope with the β-function weighted transverse impedance. Using the Gaussian beam model the corresponding form factor was replaced in agreement with [3]. Then code uses ($\perp$ stands for horizontal or vertical) :

$$\Delta\omega_\perp^m = -i\frac{N_b e}{4\pi(E/e)T_0\sigma_\tau}\frac{\Gamma(m+1/2)}{2^m m!}(\beta_\perp^{local}Z_\perp)^m_{eff} \qquad (2)$$

with E as beam energy, m as azimuthal mode number, $T_0 = 2\pi/\omega_0$ as revolution time, N_b as number of particles per bunch, M the number of bunches, ν_s as synchrotron tune, μ as coupled bunch mode number and with :

$$(\beta_\perp^{local}Z_\perp)^m_{eff} = \frac{\sum\limits_{p=-\infty}^{\infty}\beta_\perp Z_\perp(\omega_p)\cdot h_m(\omega_p-\omega_\xi)}{\sum\limits_{p=-\infty}^{\infty}h_m(\omega_p-\omega_\xi)}$$

$$\omega_p = (pM + \mu + \nu_\beta + m\nu_s)\omega_0$$

with $h_m(\omega)$ as hermitian functions and $\omega_\xi = \frac{\xi}{\eta}\omega_\beta$. The formulas were used to calculate the threshold current as a function of chromaticity. The threshold current[1] is defined if the growth rate (the imaginary part of the frequency shift in (2)) reaches the radiation damping. No Landau damping is applied. Figure 7 show that at high chromaticity the horizontal threshold is above the nominal current of 400mA. However, in order to allow the operation at low chromaticity a transverse feedback on both planes is necessary.

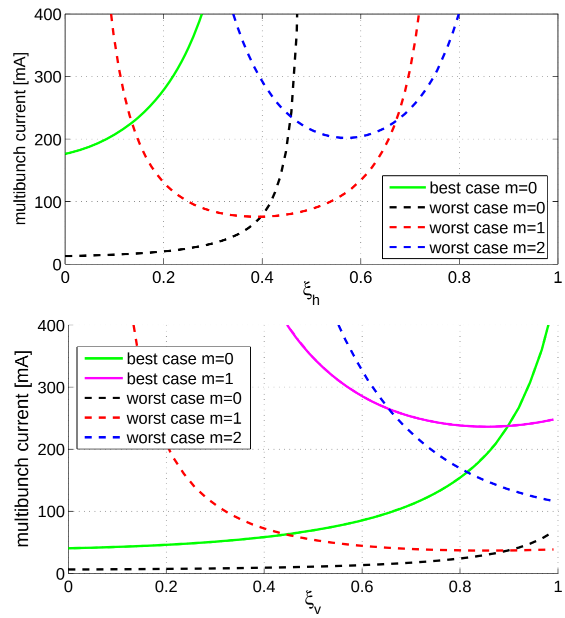

Figure 7: multibunch threshold current of different modes vs. normalized chromaticity for both cases and both planes

Table 3: effective β-function weighted transverse resistive wall impedance for different configurations (m=0, $\xi = 0$)

configuration	$\beta_H Z_H^{eff}(k\Omega)$	$\beta_V Z_V^{eff}(k\Omega)$
best case	133	383
worst case	1851	2491

REFERENCES

[1] R. L. Gluckstern, J. V. Zejits, and B. Zotter, Phys. Rev. E, **47** 1, (1993), 656

[2] M. S. Zisman, S. Chattopadhyay, J. J. Bisognano, ZAP User's Manual, LBL December 1986

[3] A. W. Chao, M. Tigner, Handbook of Accelerator Physics and Engineering, World scientific, 2^{nd} printing, p. 212

[1] the lowest threshold for different coupled bunch modes μ is taken